OMICS Journal of Radiology
ISSN: 2167-7964

Sasaki et al., OMICS J Radiol 2017, 6:5
DOI: 10.4172/2167-7964.1000276

Research Article OMICS International

Free-Breathing Hepatobiliary Phase Gd-EOB-DTPA-Enhanced MR Imaging with Radial VIBE Sequence: Comparison with Conventional Cartesian VIBE Sequence

Sasaki M[1], Fukukura Y[2]*, Kumagae Y[2], Iwanaga T[1], Saito T[1], Imai H[3], Saigo Y[1] and Yoshiura T[2]

[1]*Department of Radiological Technology, Kagoshima University Hospital, Kagoshima, Japan*
[2]*Department of Radiology, Kagoshima University Graduate School of Medical and Dental Sciences, Kagoshima, Japan*
[3]*Siemens Healthcare K. K., Tokyo, Japan*

Abstract

Purpose: To assess the feasibility of three-dimensional fat-suppressed T1-weighted gradient-echo sequence with radial volumetric interpolated breath-hold examination (rVIBE) compared with that of conventional Cartesian VIBE (cVIBE) sequence for free-breathing hepatobiliary phase of gadolinium-ethoxybenzyl-diethylenetriaminepentaacetic acid (Gd-EOB-DTPA)-enhanced MR imaging and to investigate the optimal number of radial views for rVIBE.

Methods: Thirty patients who underwent hepatobiliary phase Gd-EOB-DTPA-enhanced MR imaging with free-breathing cVIBE and rVIBE sequences using radial views of 256 ($rVIBE_{256}$), 512 ($rVIBE_{512}$), and 1024 ($rVIBE_{1024}$) for the evaluation of suspected liver tumors were enrolled in our study. Signal-to-noise ratios (SNRs) of the liver and image quality were compared between cVIBE and rVIBE sequences using the Steel-Dwass test of post hoc nonparametric multiple comparisons.

Results: SNR of the liver was significantly higher for rVIBE with all three radial views than for cVIBE (all, $P<0.001$). The $rVIBE_{256}$ showed a significantly lower SNR than $rVIBE_{512}$ ($P=0.004$) and $rVIBE_{1024}$ ($P<0.001$), but no significant difference was obtained between $rVIBE_{512}$ and $rVIBE_{1024}$ ($P=0.122$). The overall image quality was significantly higher for all rVIBE radial views than for cVIBE (all, $P<0.001$). The mean score of overall image quality was significantly lower for $rVIBE_{256}$ than for $rVIBE_{512}$ and $rVIBE_{1024}$ (both, $P<0.001$), and there was no significant difference between $rVIBE_{512}$ and $rVIBE_{1024}$ ($P=0.902$).

Conclusions: Our study suggests that $rVIBE_{512}$ is more feasible in patients with diminished respiratory capacity in the hepatobiliary phase of Gd-EOB-DTPA-enhanced MR imaging.

Keywords: Liver; Free-breathing abdominal MRI; Radial k-space sampling; Three-dimensional gradient echo-sequence; Gadoxetic acid-DTPA (Gd-EOB-DTPA)

Introduction

Gadolinium-Ethoxybenzyl-Diethylenetriaminepentaacetic Acid (Gd-EOB-DTPA) has the potential for both dynamic imaging and liver-specific static MR imaging of hepatocytes with accurate delineation and characterization of liver tumors [1-3]. Approximately half of the injected dose is taken-up by hepatocytes reaching a plateau after approximately 20 minutes and lasting for approximately 2 hours. The hepatobiliary phase of Gd-EOB-DTPA-enhanced MR imaging can visualize focal hepatic lesions with great contrast and assess liver function [1-5]. Therefore, in recent liver MR imaging, taking high quality hepatobiliary phase images is very important. However, motion artifacts such as respiratory motion, cardiac pulsation, and bowel peristalsis can degrade the image quality of abdominal MR examinations [6-8].

The breath-hold fat-saturated three-dimensional (3D) T1-weighted gradient echo sequence is usually selected for hepatobiliary phase Gd-EOB-DTPA-enhanced MR imaging because of its ability to image thin slices of the whole liver within a single acquisition and to reduce motion artifacts [6,9-11]. However, in patients with a diminished breath-hold capacity, such as elderly, debilitated, or pediatric patients, motion artifacts degrade image quality and diagnosis can become difficult [12,13].

Recently, radial volumetric interpolated breath-hold examination (rVIBE), which is a modified version of the conventional Cartesian VIBE (cVIBE) sequence, has been developed [8,14-18]. This technique uses the "stack-of-stars" scheme to acquire the k-space data and certain data consistency constraints can be applied to reduce motion artifacts [13]. Several researchers have reported that free-breathing rVIBE was feasible for abdominal MR imaging, particularly imaging patients who have difficulty holding their breath [8,17,18]. However, there is a paucity in the research on the feasibility of the rVIBE sequence for hepatobiliary phase Gd-EOB-DTPA-enhanced MR imaging [12,18]. Moreover, the optimal number of radial views for rVIBE has not been elucidated.

Therefore, the purpose of our study was to assess the feasibility of three-dimensional fat-suppressed T1-weighted gradient-echo sequence with rVIBE compared with that of cVIBE sequence for free-breathing hepatobiliary phase Gd-EOB-DTPA-enhanced MR imaging and to investigate the optimal number of radial views for rVIBE.

***Corresponding author:** Yoshihiko Fukukura, Department of Radiology, Kagoshima University Graduate School of Medical and Dental Sciences, 8-35-1 Sakuragaoka, Kagoshima City 890-8544, Japan, Tel: +81-99-275-5417; Fax: +81-99-265-1106; E-mail: yoshihiko2002jp@yahoo.co.jp

Received October 03, 2017; **Accepted** October 10, 2017; **Published** October 17, 2017

Citation: Sasaki M, Fukukura Y, Kumagae Y, Iwanaga T, Saito T, et al. (2017) Free-Breathing Hepatobiliary Phase Gd-EOB-DTPA-Enhanced MR Imaging with Radial VIBE Sequence: Comparison with Conventional Cartesian VIBE Sequence. OMICS J Radiol 6: 276. doi: 10.4172/2167-7964.1000276

Methods

Subjects and MR imaging protocols

Phantom study: Phantom imaging was performed using a 1.5-Tesla clinical system (MAGNETOM Aera, SIEMENS Healthcare GmbH, Erlangen, Germany) with body coil. 3D fat-suppressed T1-weighted gradient-echo images with cVIBE and rVIBE of a performance evaluation phantom filled with 5.3 L of phantom fluid (3.75 g $NiSO_4 \times 6H_2O$+5 g NaCl per 1000 g H_2O solution, SIEMENS Healthcare GmbH) were obtained twice, respectively. Scan parameters of cVIBE and rVIBE are shown in Table 1. The rVIBE parameters were kept the same for cVIBE. The rVIBE acquisition was divided into three subgroups: the number of radial views of 256 ($rVIBE_{256}$); 512 ($rVIBE_{512}$); and 1024 ($rVIBE_{1024}$). Acquisition time was 40 s for cVIBE, 42 s for $rVIBE_{256}$, 84 s for $rVIBE_{512}$, and 167 s for $rVIBE_{1024}$.

Clinical study: Patients were eligible for study inclusion if they:

- were suspected of having focal hepatic tumors according to previously performed ultrasonography or CT;
- were not pregnant;
- were at least 20 yrs of age; and
- had no history of anaphylactoid reaction to liver specific MRI contrast media, did not have renal failure (defined as estimated glomerular filtration rate,<30 mL/min/1.73m^2), and had no contraindication to MRI (eg. noncompatible biometallic implants or claustrophobia).

Between April and June 2015, 34 consecutive patients who met the selection criteria underwent Gd-EOB-DTPA-enhanced MR imaging. Four patients were excluded for reasons that might have affected MR imaging data, including prior hepatectomy (n=2), remarkable susceptibility artifacts (n=1), and a difficult Region of Interest (ROI) setting due to diffuse liver tumors (n=1). Finally, a total of 30 consecutive patients (17 men, 13 women; mean age, 64.6 yrs; range, 24 yrs–85 yrs) were enrolled in our study. Four patients had no suspicious discrete hepatic nodules, whereas 26 patients had hepatic nodules. These nodules were diagnosed as metastasis (n=13), hepatocellular carcinoma (n=9), hemangioma (n=2), lymphoid hyperplasia (n=1), or abscess (n=1). Eighteen patients had normal liver function with no history of liver dysfunction. Chronic liver disease was present in 12 patients. The underlying causes of chronic liver disease were hepatitis B (n=2), hepatitis C (n=3), or nonalcoholic steatohepatitis (n=2).

All MR images were obtained using a 1.5-Tesla clinical system with 18 channel body array and 32 channel spine coils. Dynamic images using 3D fat-suppressed T1-weighted gradient-echo VIBE were obtained before and after the injection of the intravenous contrast agent. In all patients, 0.025 mmol/kg body weight of Gd-EOB-DTPA (Primovist, Bayer Schering Pharma, Berlin, and Germany) was intravenously administered at a flow rate of 1 mL/s, followed by a 40 mL saline solution flush. Twenty minutes after the administration of Gd-EOB-DTPA, free-breathing cVIBE and rVIBE examinations with the radial views of 256 ($rVIBE_{256}$), 512 ($rVIBE_{512}$), and 1024 ($rVIBE_{1024}$) were obtained. Scan parameters were the same as those used in the phantom study, except for the matrix size of 208× 256 and generalized auto calibrating partially parallel acquisition with an acceleration factor of two for cVIBE (Table 2). Parallel acceleration was not used for rVIBE acquisition as it is part of the intrinsic nature of rVIBE technique.

Our routine MR imaging study included T1-weighted gradient-echo, T2-weighted turbo spin-echo, and respiratory triggered with navigator-echo technique fat-suppressed T2-weighted turbo spin-echo sequences before Gd-EOB-DTPA administration.

	cVIBE	rVIBE
TR/TE (msec)	2.75/1.32	2.75/1.32
Flip angle (°)	10	10
FOV (mm)	350	350
Matrix (phase × frequency)	256 × 256	256 × 256
Thickness (mm)	2	2
Band width (Hz/pixel)	980	980
GRAPPA	No	No
Number of excitations	1	1
Number of slices	80	80
Number of radial view	-	256
		512
		1024
Acquisition time (sec)	40	42 (256 radial views)
		84 (512 radial views)
		167 (1024 radial views)
Note: cVIBE: Conventional Cartesian VIBE; rVIBE: radial VIBE; GRAPPA: Generalized autocalibrating partially parallel acquisitions		

Table 1: Scan parameters for cVIBE and rVIBE in phantom study.

	cVIBE	rVIBE
TR/TE (msec)	2.75/1.32	2.75/1.32
Flip Angle (°)	10	10
FOV (mm)	350	350
Matrix (phase × frequency)	208 × 256	256 × 256
Thickness (mm)	2	2
Band width (Hz/pixel)	980	980
GRAPPA	2	No
Number of excitations	1	1
Number of slices	80	80
Number of radial view	-	256
		512
		1024
Acquisition time (sec)	20	42 (256 radial views)
		84 (512 radial views)
		167 (1024 radial views)
Note: cVIBE: Conventional Cartesian VIBE; rVIBE: radial VIBE; GRAPPA: Generalized autocalibrating partially parallel acquisitions		

Table 2: Scan parameters for cVIBE and rVIBE in clinical study.

Image Analysis

Phantom study

Phantom Signal-to-Noise Ratios (SNRs) for cVIBE and all rVIBE radial views were measured using the National Electrical Manufacturers Association method [19] by a radiological technologist (M.S.) who had no knowledge of the sequence parameters. In each sequence, two original phantom images were subtracted, and the subtracted image was obtained. Using the first original image, the signal intensity (SI) was measured by the mean signal intensity in ROI covering approximately 80% of the phantom. The noise was the standard deviation (SD) in the same ROI on the subtracted image. The SNR was calculated using the following equation: $SNR=\sqrt{2}\times SI/SD_{sub}$, where the factor of $\sqrt{2}$ arises because the SD is derived from the subtraction image and not from the original image.

Clinical study

Quantitative analysis: In all 30 patients, liver signal intensities on hepatobiliary phase Gd-EOB DTPA-enhanced MR images were measured by a radiologist who was blinded to the sequence parameters and clinical information. As shown in Figure 1, ROIs were placed over the lateral, medial, anterosuperior, anterioinferior, posterosuperior, and posteroinferior segments (approximately 100 mm^2) of the liver avoiding blood vessels. SNRs were calculated as SI/SD within the ROI and were averaged among six hepatic segments.

Qualitative analysis: To evaluate the image quality of cVIBE, $rVIBE_{256}$, $rVIBE_{512}$, and $rVIBE_{1024}$, two radiologists (Y.F. and Y.K., with 23 yrs and 14 yrs of experience in abdominal radiology, respectively), blinded to the sequence parameters and clinical information, independently scored the images on a 1–5 scale regarding motion artifact including streak artifact (1: extreme, 2: severe, 3: moderate, 4: mild, 5: none) and overall image quality (1: unacceptable, 2: poor, 3: acceptable, 4: good, 5: excellent), with the higher score representing the more desirable examination. For further analyses, the qualitative scores were averaged between the results of two readers.

Statistical Analysis

SNR of the liver, and the scores of the motion artifact and overall image quality were compared between cVIBE and all rVIBE radial views by using the Steel-Dwass test of post hoc nonparametric multiple comparisons. Statistical analyses were performed using JMP version 9 software (SAS Institute Japan, Tokyo, Japan). Values of $P<0.05$ were considered to indicate a significant difference.

Weighted kappa analyses were carried out to determine interobserver agreement for the motion artifact and overall image quality in cVIBE, $rVIBE_{256}$, $rVIBE_{512}$, and $rVIBE_{1024}$ (κ=0.00–0.20, poor correlation; κ=0.21–0.40, fair correlation; κ=0.41–0.60, moderate correlation; κ=0.61–0.80, good correlation; κ=0.81–1.00, excellent correlation) [20].

Results

Phantom study

The phantoms SNRs were 20.3 for cVIBE, 31.9 for $rVIBE_{256}$, 46.0 for $rVIBE_{512}$, and 69.7 for $rVIBE_{1024}$; hence, the values were higher in every rVIBE than in cVIBE. The SNR for rVIBE increased as the number of radial views increased.

Clinical study

Quantitative analysis: Mean SNRs of the liver were 12.3 ± 2.3 for cVIBE, 20.3±3.6 for $rVIBE_{256}$, 24.2 ± 4.4 for $rVIBE_{512}$, and 27.0 ± 5.3 for $rVIBE_{1024}$ (Figure 2). All rVIBE radial views showed a significant higher SNR than cVIBE (all, $P<0.001$). SNR of the liver was significantly lower for $rVIBE_{256}$ than for $rVIBE_{512}$ ($P=0.004$) and $rVIBE_{1024}$ ($P<0.001$). The $rVIBE_{1024}$ had a higher SNR than $rVIBE_{512}$, but the difference was not statistically significant ($P=0.122$).

Qualitative analysis: The results of qualitative analyses are shown in Tables 3 and 4. Interobserver agreements were excellent (κ value=0.963 for motion artifact, κ value=0.941 for overall image quality).

The scores of motion artifact were significantly higher for all rVIBE radial views than for cVIBE (all, $P<0.001$; Figure 3). The $rVIBE_{256}$ showed a significant lower score than $rVIBE_{512}$ and $rVIBE_{1024}$ (both, $P<0.001$). However, no significant difference was obtained between $rVIBE_{512}$ and $rVIBE_{1024}$ ($P=0.968$).

All three rVIBE radial views showed significantly higher scores for overall image quality than cVIBE (all, $P<0.001$; Figure 4). The mean score of the overall image quality was significantly lower for $rVIBE_{256}$ than for $rVIBE_{512}$ and $rVIBE_{1024}$ (both, $P<0.001$), and there was no significant difference between $rVIBE_{512}$ and $rVIBE_{1024}$ ($P=0.902$).

A representative case that underwent hepatobiliary phase Gd-EOB DTPA-enhanced MR imaging with cVIBE and rVIBE is shown in Figure 5.

Discussion

We sought to determine whether the quality of a free-breathing

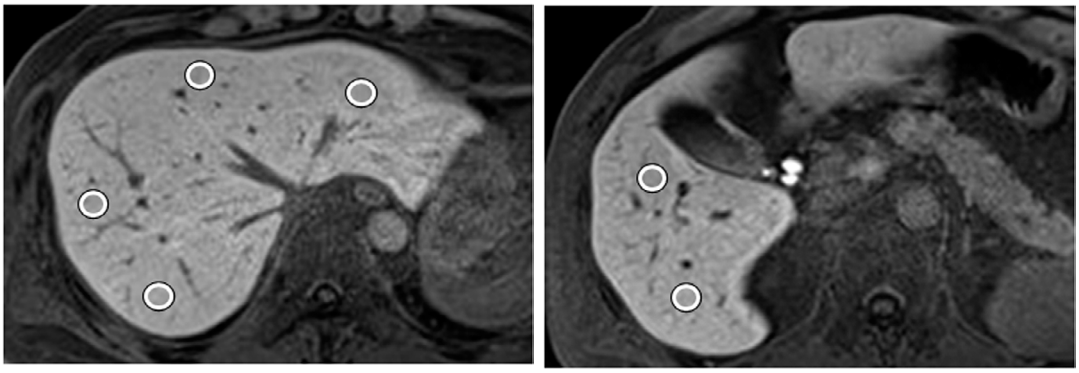

Figure 1: Hepatobiliary phase Gd-EOB-DTPA-enhanced MR image of the liver. Circles are regions of interest for signal-to-noise ratio of the lateral, medial, anterosuperior, anteroinferior, posterosuperior, and posteroinferior segments of the liver.

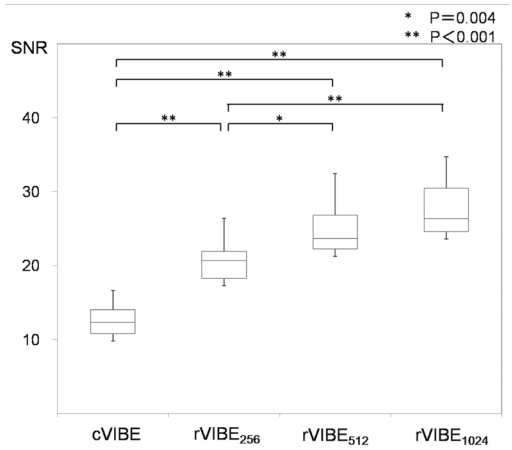

Figure 2: Signal-to-noise ratio of the liver on hepatobiliary phase gadolinium-ethoxybenzyl-diethylenetriaminepentaacetic acid-enhanced MR imaging. All three rVIBE radial views show a significantly higher SNR than cVIBE (all, P<0.001). The $rVIBE_{256}$ shows a significantly lower SNR than $rVIBE_{512}$ (P=0.004) and $rVIBE_{1024}$ (P<0.001). Note: SNR, signal-to-noise ratio; cVIBE, conventional Cartesian VIBE; $rVIBE_{256}$, radial VIBE with a radial view number of 256; $rVIBE_{512}$, radial VIBE with a radial view number of 512; $rVIBE_{1024}$, radial VIBE with a radial view number of 1024

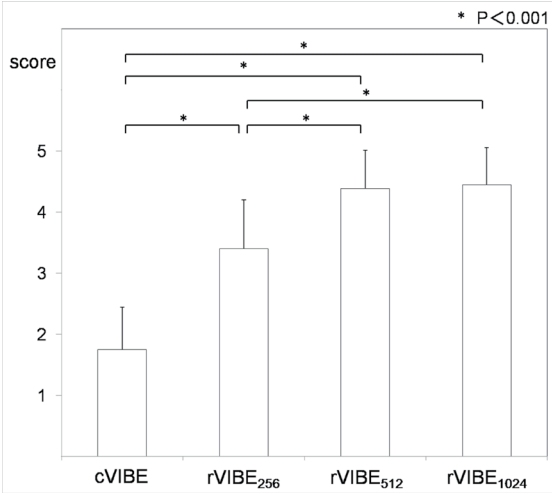

Figure 3: Visual score of motion artifact on the hepatobiliary phase gadolinium-ethoxybenzyl-diethylenetriaminepentaacetic acid-enhanced MR imaging. The scores are significantly higher for all three rVIBE radial views than for cVIBE (all, P<0.001). There is a significant difference between $rVIBE_{256}$ and $rVIBE_{512}$ or $rVIBE_{1024}$ (both, P<0.001). Note: cVIBE, conventional Cartesian VIBE; $rVIBE_{256}$, radial VIBE with a radial view number of 256; $rVIBE_{512}$, radial VIBE with a radial view number of 512; $rVIBE_{1024}$, radial VIBE with a radial view number of 1024

	Reviewer 1	Reviewer 2	Mean
cVIBE	1.73 ± 0.68	1.77 ± 0.72	1.75 ± 0.69
$rVIBE_{256}$	3.47 ± 0.81	3.33 ± 0.83	3.40 ± 0.80
$rVIBE_{512}$	4.40 ± 0.61	4.37 ± 0.66	4.38 ± 0.63
$rVIBE_{1024}$	4.47 ± 0.62	4.43 ± 0.62	4.45 ± 0.61

Note: cVIBE: Conventional Cartesian VIBE; $rVIBE_{256}$: radial VIBE with a radial view number of 256; $rVIBE_{512}$: radial VIBE with a radial view number of 512; $rVIBE_{1024}$: radial VIBE with a radial view number of 1024

Table 3: Qualitative analyses in motion artifact.

	Reviewer 1	Reviewer 2	Mean
cVIBE	1.71 ± 0.90	1.80 ± 0.79	1.75 ± 0.83
$rVIBE_{256}$	3.43 ± 0.63	3.50 ± 0.62	3.47 ± 0.61
$rVIBE_{512}$	3.99 ± 0.37	4.13 ± 0.56	4.06 ± 0.44
$rVIBE_{1024}$	4.11 ± 0.29	4.23 ± 0.50	4.17 ± 0.36

Note: cVIBE: Conventional Cartesian VIBE; $rVIBE_{256}$: radial VIBE with a radial view number of 256; $rVIBE_{512}$: radial VIBE with a radial view number of 512; $rVIBE_{1024}$: radial VIBE with a radial view number of 1024

Table 4: Qualitative analyses in overall image quality.

3D fat-suppressed T1-weighted gradient-echo sequence with rVIBE was sufficient for hepatobiliary phase Gd-EOB-DTPA-enhanced MR imaging. Our results revealed that radial k-space sampling in a free-breathing hepatobiliary phase Gd-EOB-DTPA-enhanced MR imaging leaded to a reduced motion artifact level, and demonstrated superior image quality compared to Cartesian data acquisition using objective and subjective analyses. Good interobserver agreement for the determination of the best sequence underlines this finding.

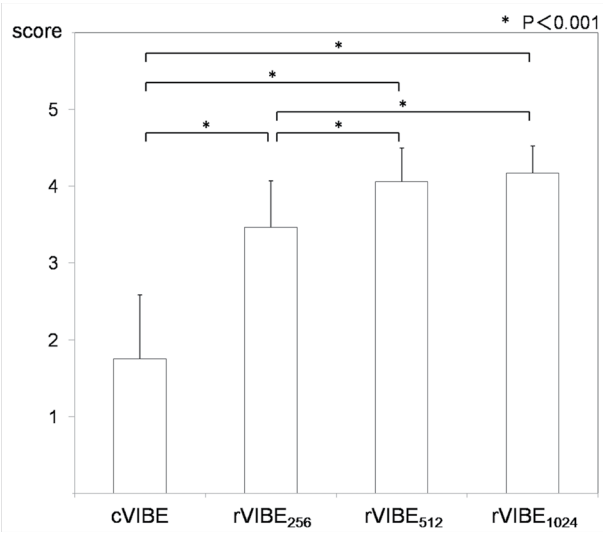

Figure 4: Visual score of overall image quality on hepatobiliary phase gadolinium-ethoxybenzyl-diethylenetriaminepentaacetic acid-enhanced MR imaging. All three rVIBE radial views show a significantly higher score for overall image quality than cVIBE (P<0.001). There is a significant difference between $rVIBE_{256}$ and $rVIBE_{512}$ or $rVIBE_{1024}$ (both, P<0.001). Note: cVIBE, conventional Cartesian VIBE; $rVIBE_{256}$, radial VIBE with a radial view number of 256; $rVIBE_{512}$, radial VIBE with a radial view number of 512; $rVIBE_{1024}$, radial VIBE with a radial view number of 1024

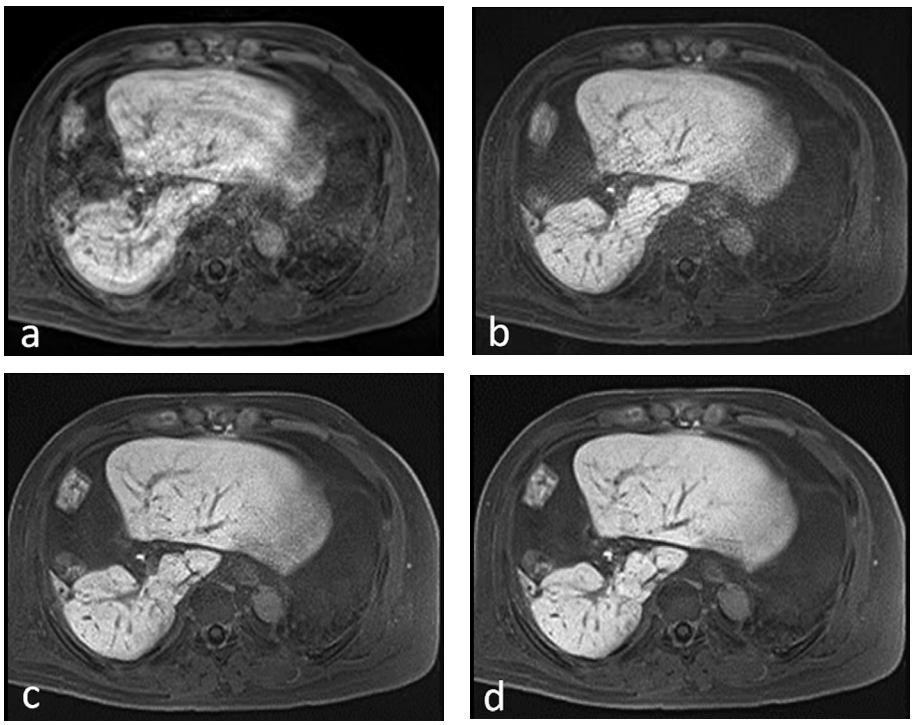

Figure 5: Hepatobiliary phase gadolinium-ethoxybenzyl-diethylenetriaminepentaacetic acid-enhanced MR imaging with hepatitis C. (a) conventional Cartesian VIBE (cVIBE), (b) radial VIBE with a radial view number of 256 ($rVIBE_{256}$), (c) radial VIBE with a radial view number of 512 ($rVIBE_{512}$), and (d) radial VIBE with a radial view number of 1024 ($rVIBE_{1024}$). cVIBE image (a) has deteriorated (score=1) for overall image quality with severe breathing motion artifacts (score=2). For the $rVIBE_{256}$ image (b), image quality improved (score=3), but with moderate motion artifacts (score=3). Images with $rVIBE_{512}$ (c) and $rVIBE_{1024}$ (d) show clear vessel border delineation with excellent image quality (score=5) because of mild (score=4) for $rVIBE_{512}$ and few motion artifacts (score=5) for $rVIBE_{1024}$.

In our phantom study, all rVIBE ($rVIBE_{256}$, 31.9; $rVIBE_{512}$, 46.0; and $rVIBE_{1024}$; 69.7) radial views showed higher SNRs than cVIBE (20.3). There have been no previous reports comparing SNR between cVIBE and rVIBE in a phantom study. Although the reasons for the higher SNR with rVIBE are unclear, the reason can be explained by the repeated acquisition around the center of k-space compared with standard Cartesian k-space readout, and uncorrected higher frequency data in kx-ky because of cylindrical shape of stack-of-stars trajectory [21-23].

Our clinical study showed that liver SNRs on hepatobiliary phase Gd-EOB-DTPA-enhanced MR images were significantly higher for

all rVIBE radial views than for cVIBE (P<0.001), as observed in our phantom study. Shin et al. [13] reported that rVIBE showed higher liver SNR on gadoteric acid-enhanced MR imaging in pediatric patients. Image quality has been reported to be significantly higher for rVIBE on abdominal MR imaging in pediatric or uncooperative patients, compared with cVIBE [8,17]. In our qualitative analyses, rVIBE reduced motion artifacts and achieved better overall image quality (p<0.001) than cVIBE on hepatobiliary phase Gd-EOB-DTPA-enhanced MR imaging. The better overall image quality of rVIBE might be attributable not only to the higher SNR because of a part of the intrinsic nature of the rVIBE technique and no use of parallel-imaging methods, but also to the reduction of widespread motion artifacts that resulted from use of radial k-space sampling. Therefore, our study indicated that rVIBE could be more useful than cVIBE for hepatobiliary phase Gd-EOB-DTPA-enhanced MR imaging, particularly in patients with diminished breath-hold capacity.

In our phantom and clinical studies, rVIBE improved SNR when we increased the number of radial views. The $rVIBE_{256}$ showed statistically poorer qualitative image quality compared with $rVIBE_{512}$ and $rVIBE_{1024}$. With conventional Cartesian k-space sampling, object motion translates into dominant motion artifacts (ghosting) along the phase-encoding direction as well as overall image blurring. Such a vulnerable phase-encoding axis does not exist in the rVIBE radial geometry, and motion artifacts present as streak artifacts with the stack-of-stars scheme where radial sampling is performed in plane [8]. One of the disadvantages of radial k-space sampling is streak artifacts [17]. Kim et al. [24] reported that decreasing the number of radial views leads to an increase in streaking artifacts. Block et al. [25] reported that the rVIBE sequence should be used with radial view numbers of 400–800 when using matrix sizes of 224-384 in free-breathing abdominal MR imaging. In our study using the matrix size of 256 × 256, motion artifacts were remarkable on the image with the radial view number of 256 ($rVIBE_{256}$), and these artifacts improved when using the radial view numbers of 512 ($rVIBE_{512}$) or 1024 ($rVIBE_{1024}$). Therefore, the inferior image quality on $rVIBE_{256}$ compared with $rVIBE_{512}$ or $rVIBE_{1024}$ was considered to be due to the insufficient number of radial views compared with the matrix size, which would cause the streak artifact with radial sampling.

As the number of radial views increased, the data acquisition time became longer, although SNR improved with less motion artifacts. In our study, data acquisition times were 84 s for $rVIBE_{512}$ and 167 s for $rVIBE_{1024}$. Moreover, no significant difference between $rVIBE_{512}$ and $rVIBE_{1024}$ was obtained in quantitative (P=0.122) or qualitative analyses (P=0.968 for motion artifact and 0.902 for overall image quality). A shorter acquisition time would be desirable in a busy clinical setting. Therefore, our study suggested that $rVIBE_{512}$ might be more convenient for hepatobiliary phase Gd-EOB-DTPA-enhanced MR imaging compared with $rVIBE_{1024}$ because of the shorter examination time.

Our study has several limitations. First, our study includes a relatively small number of patients. Nevertheless, our results suggested that rVIBE might have fewer artifacts and higher overall image quality than cVIBE for liver imaging in patients with diminished breath-hold capacity. Second, we did not assess the visualization of liver lesions on hepatobiliary phase Gd-EOB-DTPA-enhanced MR imaging with cVIBE or rVIBE, and thus, we cannot definitively state the usefulness of rVIBE for detecting liver tumors. However, we believe that higher SNR and better image quality would yield better visualization of liver tumors.

Conclusion

Our results demonstrated that data acquisition using radial k-space sampling reduced motion artifacts, and thus improved robustness for motion. The radial view number of 512 was considered to be more suitable for hepatobiliary phase Gd-EOB-DTPA-enhanced MR imaging when using a matrix size of 256 × 256. The rVIBE acquisitions were longer than cVIBE because parallel-imaging methods, which are widely used with cVIBE, have not been established for rVIBE. However, we believe it is possible to add the rVIBE sequence to the scanning protocol in the setting of non-cooperative patients for hepatobiliary phase Gd-EOB-DTPA-enhanced MR imaging, and the rVIBE sequence could be useful for detection and characterization of liver tumors and evaluation of liver function.

Acknowledgement

We wish to thank the staff of the Department of Radiology and the Joint Research Laboratory, Kagoshima University Graduate School of Medical and Dental Sciences, for the use of their facilities.

Competing Interests

The authors declare that they have no competing interests.

Ethics Approval and Consent to Participate

This study was approved by the institutional review board of Kagoshima University Hospital (approval No. 27-74). All procedures performed in studies involving human participants were in accordance with the ethical standards of the institutional and/or national research committee and with the 1964 Helsinki declaration and its later amendments or comparable ethical standards.

References

1. Bluemke DA, Sahani D, Amendola M, Balzer T, Breuer J, et al. (2005) Efficacy and safety of MR imaging with liver-specific contrast agent: U.S. multicenter phase III study. Radiology 237: 89-98.
2. Hammerstingl R, Huppertz A, Breuer J, Balzer T, Blakeborough A, et al. (2008) Diagnostic efficacy of gadoxetic acid (Primovist)-enhanced MRI and spiral CT for a therapeutic strategy: Comparison with intraoperative and histopathologic findings in focal liver lesions. Eur Radiol 18: 457-467.
3. Yoneyama T, Fukukura Y, Kamimura K, Takumi K, Umanodan A, et al. (2014) Efficacy of liver parenchymal enhancement and liver volume to standard liver volume ratio on Gd-EOB-DTPA-enhanced MRI for estimation of liver function. Eur Radiol 24: 857-865.
4. Ba-Ssalamah A, Uffmann M, Saini S, Bastati N, Herold C, et al. (2009) Clinical value of MRI liver-specific contrast agents: A tailored examination for a confident non-invasive diagnosis of focal liver lesions. Eur Radiol 19: 342-357.
5. Yamada A, Hara T, Li F, Fujinaga Y, Ueda K, et al. (2011) Quantitative evaluation of liver function with use of Gadoxetate disodium-enhanced MR imaging. Radiology 260: 727-733.
6. Kim BS, Lee KR, Goh MJ (2014) New imaging strategies using a motion-resistant liver sequence in uncooperative patients. BioMed Res Int 2014: 1-11.
7. Chandarana H, Block TK, Rosenkrantz AB, Lim RP, Kim D, et al. (2011) Free-breathing radial 3D fat-suppressed T1-weighted gradient echo sequence. Invest Radiol 46: 648-653.
8. Chandarana H, Block TK, Winfeld MJ, Lala SV, Mazori D, et al. (2014) Free-breathing contrast-enhanced T1-weighted gradient-echo imaging with radial k-space sampling for paediatricabdominopelvic MRI. Eur Radiol 24: 320-326.
9. Rofsky NM, Lee VS, Laub G, Pollack MA, Krinsky GA, et al. (1999) Abdominal MR imaging with a volumetric interpolated breath-hold examination. Radiology 212: 876-884.
10. McKenzie CA, Lim D, Ransil BJ, Morrin M, Pedrosa I, et al. (2004) Shortening MR image acquisition time for volumetric interpolated breath-hold examination with a recently developed parallel imaging reconstruction technique: clinical feasibility. Radiology 230: 589-594.
11. Vogt FM, Antoch G, Hunold P, Maderwald S, Ladd ME, et al. (2005) Parallel acquisition techniques for accelerated volumetric interpolated breath-hold examination magnetic resonance imaging of the upper abdomen: assessment of image quality and lesion conspicuity. J Magn Reson Imaging 21: 376-382.

12. Reiner CS, Neville AM, Nazeer HK, Breault S, Dale BM, et al. (2013) Contrast-enhanced free-breathing 3D T1-weighted gradient-echo sequence for hepatobiliary MRI in patients with breath-holding difficulties. Eur Radiol 23: 3087-3093.

13. Shin HJ, Kim MJ, Lee MJ, Kim HG (2016) Comparison of image quality between conventional VIBE and radial VIBE in free-breathing paediatric abdominal MRI. Clin Radiol 71: 1044-1049.

14. Song HK, Dougherty L (2004) Dynamic MRI with projection reconstruction and KWIC processing for simultaneous high spatial and temporal resolution. Magn Reson Med 52: 815-824.

15. Lin W, Guo J, Rosen MA, Song HK (2008) Respiratory motion-compensated radial dynamic contrast-enhanced (DCE)-MRI of chest and abdominal lesions. Magn Reson Med 60: 1135-1146.

16. Azevedo RM, de Campos RO, Ramalho M, Heredia V, Dale BM, et al. (2011) Free-breathing 3D T1-weighted gradient-echo sequence with radial data sampling in abdominal MRI: preliminary observations. AJR Am J Roentgenol 197: 650-657.

17. Bamrungchart S, Tantaway EM, Midia EC, Hernandes MA, Srirattanapong S, et al. (2013) Free breathing three-dimensional gradient echo-sequence with radial data sampling (Radial 3D-GRE) examination of the pancreas: Comparison with standard 3D-GRE Volumetric Interpolated Breathhold Examination (VIBE). J Magn Reson Imaging 38: 1572-1577.

18. Gomi T, Nagamoto M, Hasegawa M, Tabata A, Iwasaki M, et al. (2014) Radial MRI during free breathing in contrast-enhanced hepatobiliary phase imaging. Acta Radiol 55: 3-7.

19. National Electrical Manufacturers Association (NEMA) (2008) Determination of signal-to-noise ratio (SNR) in diagnostic magnetic resonance imaging. NEMA Standards Publication MS 1-2008 (R2014).

20. Cohen J (1968) Weighted kappa: Nominal scale agreement with provision for scaled disagreement or partial credit. Psychol Bull 70: 213-220.

21. Michaely HJ, Kramer H, Weckbach S, Dietrich O, Reiser MF, et al. (2008) Renal T2-weighted Turbo-Spin-Echo imaging with BLADE at 3.0 Tesla: Initial experience. J Magn Reson Imaging 27: 148-153.

22. Wintersperger BJ, Runge VM, Biswas J, Nelson CB, Stemmer A, et al. (2006) Brain Magnetic Resonance Imaging at 3 Tesla using BLADE compared with standard rectilinear data sampling. Invest Radiol 41: 586-592.

23. Ichinoseki Y, Nagasaka T, Miyamoto K, Tamura H, Mori I, et al. (2015) Noise power spectrum in PROPELLER MR imaging. Magn Reson Med Sci 14: 235-242.

24. Kim KW, Lee JM, Jeon YS, Kang SE, Baek JH, et al. (2013) Free-breathing dynamic contrast-enhanced MRI of the abdomen and chest using a radial gradient echo sequence with K-space weighted image contrast (KWIC). Eur Radiol 23: 1352-1360.

25. Block KT, Chandarana H, Milla S, Bruno M, Mulholland T, et al. (2014) Towards routine clinical use of radial stack-of-stars 3D gradient-echo sequences for reducing motion sensitivity. J Korean Soc Magn Reson Med 18: 87-106.